

# Controlling Electrical Conductance through a $\pi$ -Conjugated Cruciform Molecule by Selective Anchoring to Gold Electrodes

Cancan Huang, Songjie Chen, Kristian Baruël Ørnsø, David Reber, Masoud Baghernejad, Yongchun Fu, Thomas Wandlowski, Silvio Decurtins, Wenjing Hong,\*  
Kristian Sommer Thygesen,\* and Shi-Xia Liu\*

**Abstract:** Tuning charge transport at the single-molecule level plays a crucial role in the construction of molecular electronic devices. Introduced herein is a promising and operationally simple approach to tune two distinct charge-transport pathways through a cruciform molecule. Upon *in situ* cleavage of triisopropylsilyl groups, complete conversion from one junction type to another is achieved with a conductance increase by more than one order of magnitude, and it is consistent with predictions from *ab initio* transport calculations. Although molecules are well known to conduct through different orbitals (either HOMO or LUMO), the present study represents the first experimental realization of switching between HOMO- and LUMO-dominated transport within the same molecule.

The idea to integrate individual molecules into electronic circuits was theoretically proposed by Aviram and Ratner in 1974.<sup>[1]</sup> Despite various experimental approaches employed for the formation of molecular junctions between two metal electrodes,<sup>[2]</sup> it is highly desirable to incorporate a third (gate) electrode, for example, a solid-state back gate electrode<sup>[3]</sup> or electrochemical electrode, to adjust molecular energy levels relative to the Fermi level or trigger redox reactions on the molecule.<sup>[4]</sup> In conjunction with this idea, it is of great interest to integrate molecules with multiple terminals into an electrical circuit to allow differentiating and switching between different charge-transport pathways. However, it still remains a challenge to control the metal–molecule contact to a degree that allows the injection/extraction of charges at different points of the same molecule and thereby explore multiple electron pathways. A possible way to overcome this challenge is to exploit the sizeable variation in binding energies of different anchor groups on a gold surface.

Herein, we report the design and synthesis of a cruciform conjugated molecule (**M1**) consisting of two orthogonally disposed  $\pi$ -systems. Within this molecule the two linear arms are terminated with pyridyl and TIPS-protected (TIPS = triisopropylsilyl) acetylene groups, respectively (Figure 1). Cru-

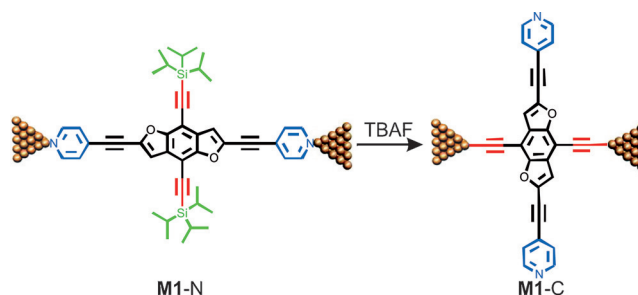


**Figure 1.** Setting a course for molecular conductance along different pathways based on the **M1-N** and **M1-C** configurations.

ciform molecules have received significant attention because of their special structural topology and opportunities for their modulation,<sup>[5]</sup> and therefore they are considered to be promising “hub” units for the integration of different functional units in single-molecule circuits. Within the context of the single-molecule conductance, only three papers on cruciform molecules have appeared in the literature.<sup>[6,7]</sup> Differentiating charge-transport pathways, however, has been unexplored so far. To elaborate on our concept for achieving high selectivity of anchoring sites on gold leads, we apply desilylation chemistry,<sup>[8]</sup> which allows trapping of molecules between two gold electrodes through *in situ* generated C–Au bonds. Single-molecule junctions formed by the C–Au  $\sigma$ -bonds should be energetically favored over junctions through pyridyl anchoring groups, because of the larger binding strength of the covalent bond compared to the coordinative bonding between the gold and lone pair atoms.<sup>[9]</sup> Therefore, one can set the course for a controllable conductance pathway in a molecule, for example, with well-studied pyridyl and trimethylsilyl-protected acetylene termini.<sup>[4a,9]</sup>

To realize this goal, we specifically synthesized the cruciform molecule **M1** (Figure 1) based on the benzo[1,2-*b*:4,5-*b'*]difuran (BDF) core<sup>[10]</sup> to explore the possibility of chemical tuning of anchoring sites in single-molecule devices. Charge-transport properties of the single-molecule junctions before and after the desilylation were investigated using the mechanically controllable break junction technique

[\*] C. Huang,<sup>[†]</sup> Dr. S. Chen,<sup>[†]</sup> D. Reber, M. Baghernejad, Dr. Y. Fu, Prof. T. Wandlowski, Prof. S. Decurtins, Dr. W. Hong, Dr. S.-X. Liu  
Department of Chemistry and Biochemistry, University of Bern  
Freiestrasse 3, 3012 Bern (Switzerland)  
E-mail: hong@dcf.unibe.ch  
liu@dcf.unibe.ch

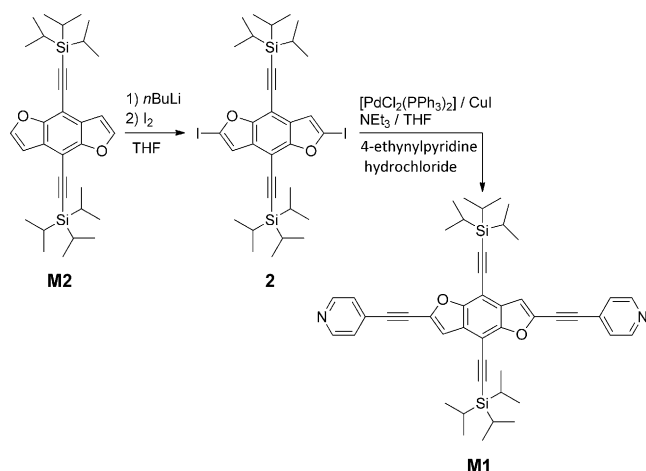
K. Baruël Ørnsø, Prof. K. S. Thygesen  
Center for Atomic-scale Materials Design (CAMD), Department of  
Physics, Technical University of Denmark  
Fysikvej, 2800 Kgs. Lyngby (Denmark)  
E-mail: thygesen@fysik.dtu.dk

[†] These authors contributed equally to this work.

Supporting information for this article is available on the WWW under <http://dx.doi.org/10.1002/anie.201506026>.

(MCBJ).<sup>[11]</sup> Upon desilylation, the conductance value is more than one order of magnitude higher, and is comparable with other conductance tuning approaches through energy level tuning or redox processes. In the present study, the origin of the conductance difference lies in a complete conversion of two charge-transport pathways in a well-controlled way, as confirmed by density functional theory based transport calculations.

As illustrated in Scheme 1, the target molecule **M1** was readily prepared from **2** in 69% yield by a Sonogashira reaction with 4-ethynylpyridine hydrochloride. The synthesis of **2** was accomplished in 54% yield by iodination of **M2**<sup>[12]</sup> through a double deprotonation in the presence of *n*BuLi and subsequent treatment with iodine. The details are given in the Supporting Information.



**Scheme 1.** Synthetic route to the target molecule **M1**.

The initial single-molecule conductance measurement was carried out in a THF/mesitylene solution (1:4, v/v) containing 0.1 mM **M1**, and then tetrabutylammonium fluoride (TBAF) was added for in situ cleavage of TIPS to form the Au–C bonds. Figure 2A displays typical conductance (*G*) versus distance ( $\Delta z$ ) stretching traces, as plotted in a semi-logarithmic scale. In these traces, after the rupture of gold–gold atomic contacts (plateau at  $G_0 = 2e^2h$ , quantum conductance), the formation of molecular junctions is identified by the presence of additional plateaus in the range  $10^{-0.3} G_0 \geq$

$G \geq 10^{-7.0} G_0$ . Some typical traces are shown for pyridyl-terminated junctions **M1-N** (blue) in the initial state and the acetylide-terminated junctions **M1-C** (red), upon the cleavage of TIPS. The plateau length of **M1-N** is significantly longer than that of **M1-C**, while the plateau of **M1-C** is in the higher conductance regime.

Thousands of these individual traces are used to construct one-dimensional (1D) conductance histograms without data selection<sup>[11a]</sup> (Figure 2B). In the initial state (blue curve), the conductance peak centered at  $G = 10^{-5.1 \pm 0.1} G_0$  is assigned as the statistically most probable conductance of the **M1-N** molecular junctions. Upon the addition of 2 equivalents of TBAF, a distinct conductance was detected at  $G = 10^{-3.9 \pm 0.1} G_0$ . The observed increase in molecular conductance is attributed to the **M1-C** charge-transport pathway. It is also found that the conductance of the **M1-C** configuration is in perfect agreement with the molecular junction of the reference molecule **M2-C** (Scheme 1;  $G = 10^{-4.0 \pm 0.1} G_0$ ), which features only one charge-transport pathway through the 4,8-axis of the BDF core. For **M2**, we applied desilylation chemistry to form the **M2-C** junction through Au–C bonds. Remarkably, the difference in conductance between the two different pathways of the cruciform molecule is comparable to the conductance variations previously obtained by gating of the molecular junctions (Fermi level tuning<sup>[13]</sup> or redox processes<sup>[14]</sup>).

For **M1**, the **M1-N** and **M1-C** configurations lead to a significant change of the molecular lengths of the single-molecule junctions. To further explore the evolution of conductance as a function of the molecular length, the two-dimensional (2D) histograms are displayed in Figure 3. Two

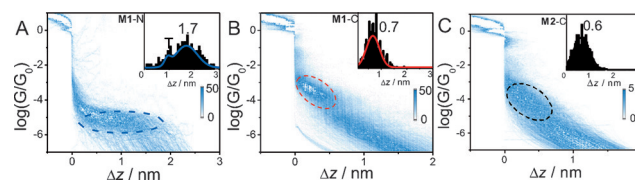


**Figure 3.** Two-dimensional (2D) conductance histograms and stretching distance  $\Delta z$  distributions (inset) of **M1-N** (A), **M1-C** (B), and **M2-C** (C). The stretching distance of the molecular junction is determined from the conductance region set between the breaking of the gold–gold atomic contact and the end of molecular plateau:  $10^{-6.0} G_0$  to  $10^{-0.3} G_0$  for **M1-N**,  $10^{-4.5} G_0$  to  $10^{-0.3} G_0$  for **M1-C**,  $10^{-4.5} G_0$  to  $10^{-0.3} G_0$  for **M2-C**.

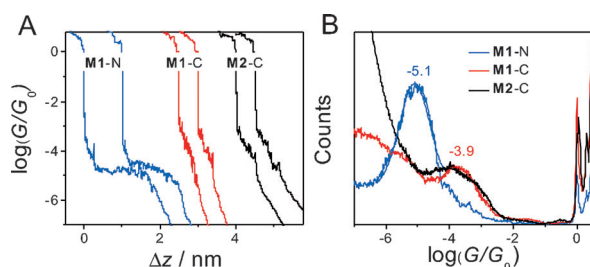


**Figure 2.** A) Typical conductance. Relative distance traces for **M1-N** and **M1-C** configurations, as well as for **M2-C**. B) One-dimensional (1D) conductance histograms of **M1-N**, **M1-C**, and **M2-C**.

clear intensity clouds are observed for **M1-N** (Figure 3A) and **M1-C** configurations (Figure 3B). Notably, the plateau length for **M1-N** is longer than for **M1-C**. The most probable stretched distance,  $\Delta z^*$ , was determined from the maximum peak position in the stretching distance ( $\Delta z$ ) distribution histograms (inset histograms of Figure 3A and B) to be 1.7 nm and 0.7 nm, respectively. After adding the snap-back distance correction, the most probable absolute distance,  $z^*$  ( $z^* = \Delta z^* + 0.5$  nm),<sup>[11b]</sup> between two gold tips is 2.2 nm for **M1-N** and 1.2 nm for **M1-C**, and it agrees well with the length of the corresponding orientations (2.4 nm for **M1-N** and 1.2 nm for **M1-C** cells based on DFT calculations). The good

agreement between the experimentally and theoretically determined junction lengths verifies the proposed junction configurations. It is interesting that the conductance plateaus of both **M1-C** and **M2-C** decrease in a continuous fashion (close to linear on the log scale) as a function of the junction length, whereas **M1-N** shows a constant plateau followed by a more abrupt jump to very low conductance. Lambert et al. studied the stretching process of the Au–C interaction.<sup>[15]</sup> It is suggested that a single gold atom is detached from the rest of the surface while the Au–C bond does not break during the stretching process, thus leading to the sharp decrease in the conductance within a short distance and thus to the tilted molecular plateaus. All these results provide direct evidence for the chemically stimulated change of the charge-transport pathway from **M1-N** to **M1-C**. In other words, depending upon the orientation of the benzodifuran backbone, the lateral interaction of the molecule with the junction electrodes changes completely. Although this issue has been intensively addressed, our observations definitely open up exciting vistas of molecular electronics.

It can be noted that the peak located at 1.7 nm, corresponding to the **M1-N** junction (inset Figure 3A), disappeared completely for the **M1-C** junction (inset Figure 3B), thus indicating that the conversion from the **M1-N** into **M1-C** charge-transport pathway can reach up to about 100 % (9 in 1000 traces which show stretching distances longer than 1.5 nm). Such a high selectivity is attributed to the fact that the covalent C–Au bonds are much stronger than the Au–N bond, as confirmed by DFT calculations. The binding energies for the pyridyl and acetylide groups on the gold electrodes are calculated to be 0.6 eV and 3.2 eV, respectively. The DFT total energy calculations were performed with the GPAW code<sup>[16b]</sup> using a real space grid with grid spacing of 0.18 Å and the PBE exchange-correlation functional. The atomic structure of the metal–molecule interface was modeled as described in the Supporting Information.

Figure 4 shows the transmission functions for **M1-N** and **M1-C** as calculated from DFT. The charge-transport calculation was performed using the GPAW electric structure

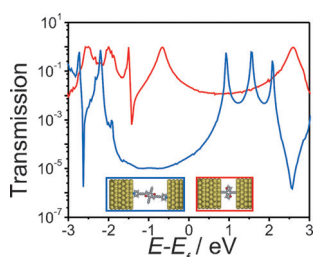


**Figure 4.** Calculated transmission function for the two states of the molecular junctions (blue for **M1-N** and red for **M1-C**).

code,<sup>[16]</sup> using a double zeta plus polarization (DZP) basis set and the PBE exchange-correlation functional. To overcome the well-known problem of DFT to describe molecular energy levels we have used the DFT + Sigma scheme to correct the DFT eigenvalues as described in previous studies.<sup>[17]</sup> As illustrated in Figure 4, the charge transport is predominantly

by the LUMO for the **M1-N** configuration and the HOMO for the **M1-C** configuration. The switching of the dominant molecular orbital is in good agreement with previous theoretical studies.<sup>[11b,15]</sup>

In summary, two distinct charge-transport pathways of a cruciform molecule are verified by single-molecule conductance measurements using the MCBJ technique, and show a conductance difference of more than one order of magnitude. Upon in situ cleavage of the TIPS groups, the complete conversion from the **M1-N** junctions into the **M1-C** junctions could be achieved. More importantly, the conductance tuning by the high selectivity of different anchoring groups provides a unique flexibility in the function modulation of devices. The interpretation of the experiments was supported by ab initio total energy and transport calculations. Although molecules are well known to conduct through different orbitals (either HOMO or LUMO), the present study represents the first experimental realization of such switching between HOMO- and LUMO-dominated transport within the same molecule.

## Acknowledgements

This work was generously supported by the Swiss National Science Foundation (grant No. 200020-144471 and 200021-147143; NFP 62), the EC FP7 ITN “MOLESCO” project number 606728, and the University of Bern. K.B.Ø. and K.S.T. thank the Danish Council for Independent Research’s DFF Sapere Aude program (grant No. 11-1051390) for financial support.

**Keywords:** ab initio calculations · conducting materials · gold · molecular electronics · single-molecule studies

**How to cite:** *Angew. Chem. Int. Ed.* **2015**, *54*, 14304–14307  
*Angew. Chem.* **2015**, *127*, 14512–14515

- [1] A. Aviram, M. A. Ratner, *Chem. Phys. Lett.* **1974**, *29*, 277–283.
- [2] a) R. C. Chiechi, E. A. Weiss, M. D. Dickey, G. M. Whitesides, *Angew. Chem. Int. Ed.* **2008**, *47*, 142–144; *Angew. Chem.* **2008**, *120*, 148–150; b) W. Haiss, H. van Zalinge, S. J. Higgins, D. Bethell, H. Höbenreich, D. J. Schiffrin, R. J. Nichols, *J. Am. Chem. Soc.* **2003**, *125*, 15294–15295; c) M. A. Reed, C. Zhou, C. J. Muller, T. P. Burgin, J. M. Tour, *Science* **1997**, *278*, 252–254; d) B. Xu, N. J. Tao, *Science* **2003**, *301*, 1221–1223.
- [3] H. Song, Y. Kim, Y. H. Jang, H. Jeong, M. A. Reed, T. Lee, *Nature* **2009**, *462*, 1039–1043.
- [4] a) C. Huang, A. V. Rudnev, W. Hong, T. Wandlowski, *Chem. Soc. Rev.* **2015**, *44*, 889–901; b) X. Xiao, D. Brune, J. He, S. Lindsay, C. B. Gorman, N. Tao, *Chem. Phys.* **2006**, *326*, 138–143.
- [5] a) J. E. Klare, G. S. Tulevski, K. Sugo, A. de Picciotto, K. A. White, C. Nuckolls, *J. Am. Chem. Soc.* **2003**, *125*, 6030–6031; b) J. N. Wilson, U. H. F. Bunz, *J. Am. Chem. Soc.* **2005**, *127*, 4124–4125; c) A. J. Zuccherro, P. L. McGrier, U. H. F. Bunz, *Acc. Chem. Res.* **2010**, *43*, 397–408; d) M. A. Saeed, H. T. M. Le, O. Š. Miljanić, *Acc. Chem. Res.* **2014**, *47*, 2074–2083.
- [6] S. Grunder, R. Huber, S. Wu, C. Schönenberger, M. Calame, M. Mayor, *Eur. J. Org. Chem.* **2010**, 833–845.
- [7] a) C. R. Parker, Z. Wei, C. R. Arroyo, K. Jennum, T. Li, M. Santella, N. Bovet, G. Zhao, W. Hu, H. S. J. van der Zant, M. Vanin, G. C. Solomon, B. W. Laursen, K. Nørgaard, M. B. Nielsen, *Adv. Mater.* **2013**, *25*, 405–409; b) C. R. Parker, E.

- Leary, R. Frisenda, Z. Wei, K. S. Jennum, E. Glibstrup, P. B. Abrahamsen, M. Santella, M. A. Christensen, E. A. Della Pia, T. Li, M. T. Gonzalez, X. Jiang, T. J. Morsing, G. Rubio-Bollinger, B. W. Laursen, K. Nørgaard, H. van der Zant, N. Agrait, M. B. Nielsen, *J. Am. Chem. Soc.* **2014**, *136*, 16497–16507.
- [8] a) Y. Fu, S. Chen, A. Kuzume, A. Rudnev, C. Huang, V. Kaliginedi, M. Baghernejad, W. Hong, T. Wandlowski, S. Decurtins, S.-X. Liu, *Nat. Commun.* **2015**, *6*, 6403; b) W. Hong, H. Li, S.-X. Liu, Y. Fu, J. Li, V. Kaliginedi, S. Decurtins, T. Wandlowski, *J. Am. Chem. Soc.* **2012**, *134*, 19425–19431.
- [9] E. Leary, A. La Rosa, M. T. Gonzalez, G. Rubio-Bollinger, N. Agrait, N. Martin, *Chem. Soc. Rev.* **2015**, *44*, 920–942.
- [10] a) C. Yi, C. Blum, M. Lehmann, S. Keller, S.-X. Liu, G. Frei, A. Neels, J. Hauser, S. Schürch, S. Decurtins, *J. Org. Chem.* **2010**, *75*, 3350–3357; b) H. Li, P. Jiang, C. Yi, C. Li, S.-X. Liu, S. Tan, B. Zhao, J. Braun, W. Meier, T. Wandlowski, S. Decurtins, *Macromolecules* **2010**, *43*, 8058–8062.
- [11] a) W. Hong, H. Valkenier, G. Meszaros, D. Z. Manrique, A. Mishchenko, A. Putz, P. M. Garcia, C. J. Lambert, J. C. Hummelen, T. Wandlowski, *Beilstein J. Nanotechnol.* **2011**, *2*, 699–713; b) W. Hong, D. Z. Manrique, P. Moreno-Garcia, M. Gulcur, A. Mishchenko, C. J. Lambert, M. R. Bryce, T. Wandlowski, *J. Am. Chem. Soc.* **2012**, *134*, 2292–2304.
- [12] Y. Aeschi, H. Li, Z. Cao, S. Chen, A. Amacher, N. Bieri, B. Özen, J. Hauser, S. Decurtins, S. Tan, S.-X. Liu, *Org. Lett.* **2013**, *15*, 5586–5589.
- [13] a) M. Baghernejad, D. Z. Manrique, C. Li, T. Pope, U. Zhurav, I. Pobelov, P. Moreno-Garcia, V. Kaliginedi, C. Huang, W. Hong, C. Lambert, T. Wandlowski, *Chem. Commun.* **2014**, *50*, 15975–15978; b) R. J. Brooke, C. Jin, D. S. Szumski, R. J. Nichols, B.-W. Mao, K. S. Thygesen, W. Schwarzacher, *Nano Lett.* **2015**, *15*, 275–280; c) B. Capozzi, Q. Chen, P. Darancet, M. Kotiuga, M. Buzzeo, J. B. Neaton, C. Nuckolls, L. Venkataraman, *Nano Lett.* **2014**, *14*, 1400–1404.
- [14] a) N. Darwish, I. Díez-Pérez, P. Da Silva, N. Tao, J. J. Gooding, M. N. Paddon-Row, *Angew. Chem. Int. Ed.* **2012**, *51*, 3203–3206; *Angew. Chem.* **2012**, *124*, 3257–3260; b) Z. Li, H. Li, S. Chen, T. Froehlich, C. Yi, C. Schönenberger, M. Calame, S. Decurtins, S.-X. Liu, E. Borguet, *J. Am. Chem. Soc.* **2014**, *136*, 8867–8870; c) X.-S. Zhou, L. Liu, P. Fortgang, A.-S. Lefevre, A. Serra-Muns, N. Raouafi, C. Amatore, B.-W. Mao, E. Maisonhaute, B. Schöllhorn, *J. Am. Chem. Soc.* **2011**, *133*, 7509–7516.
- [15] R. C. Hoft, M. J. Ford, V. M. García-Suárez, C. J. Lambert, M. B. Cortie, *J. Phys. Condens. Matter* **2008**, *20*, 025207.
- [16] a) M. Baghernejad, X. Zhao, K. Baruël Ørnsø, M. Füeg, P. Moreno-García, A. V. Rudnev, V. Kaliginedi, S. Vesztergom, C. Huang, W. Hong, P. Broekmann, T. Wandlowski, K. S. Thygesen, M. R. Bryce, *J. Am. Chem. Soc.* **2014**, *136*, 17922–17925; b) J. Enkovaara, C. Rostgaard, J. J. Mortensen, J. Chen, M. Dulak, L. Ferrighi, J. Gavnholt, C. Glinsvad, V. Haikola, H. A. Hansen, H. H. Kristoffersen, M. Kuisma, A. H. Larsen, L. Lehtovaara, M. Ljungberg, O. Lopez-Acevedo, P. G. Moses, J. Ojanen, T. Olsen, V. Petzold, N. A. Romero, J. Stausholm-Møller, M. Strange, G. A. Tritsaris, M. Vanin, M. Walter, B. Hammer, H. Häkkinen, G. K. H. Madsen, R. M. Nieminen, J. K. Nørskov, M. Puska, T. T. Rantala, J. Schiøtz, K. S. Thygesen, K. W. Jacobsen, *J. Phys. Condens. Matter* **2010**, *22*, 253202.
- [17] a) D. J. Mowbray, G. Jones, K. S. Thygesen, *J. Phys. Chem.* **2008**, *112*, 111103; b) S. Y. Quek, L. Venkataraman, H. J. Choi, S. G. Louie, M. S. Hybertsen, J. B. Neaton, *Nano Lett.* **2007**, *7*, 3477–3482.

Received: July 1, 2015

Revised: August 13, 2015

Published online: October 7, 2015